Earth Sciences
2022; 11(3): 79-88
http://www.sciencepublishinggroup.com/j/earth
doi: 10.11648/j.earth.20221103.14
ISSN: 2328-5974 (Print); ISSN: 2328-5982 (Online)

Geological and Geo-electrical Outlining of Graphite Deposits Within Kagara, North-Central Nigeria

Christopher Imoukhai Unuevho[1, *], Akobundu Nwanosike Amadi[1], Stephen Jude Ejepu[1], Emmanuel Emeka Udensi[2]

[1]Department of Geology, School of Physical Sciences, Federal University of Technology, Minna, Nigeria

[2]Department of Physics, School of Physical Sciences, Federal University of Technology, Minna, Nigeria

Email address:

c.unuevho@futminna.edu.ng (C. I. Unuevho), geoana76@gmail.com (A. N. Amadi), ejepu.jude@futminna.edu.ng (S. J. Ejepu), emmanuel.udensi@futminna.edu.ng (E. E. Udensi)

[*]Corresponding author

To cite this article:

Christopher Imoukhai Unuevho, Akobundu Nwanosike Amadi, Stephen Jude Ejepu, Emmanuel Emeka Udensi. Geological and Geo-electrical Outlining of Graphite Deposits Within Kagara, North-Central Nigeria. *Earth Sciences*. Vol. 11, No. 3, 2022, pp. 79-88. doi: 10.11648/j.earth.20221103.14

Received: April 23, 2022; **Accepted**: May 17, 2022; **Published**: May 31, 2022

Abstract: The specific locations of graphite exposures in Kagara, their host rocks, as well as their spatial extent and gross volume have hitherto remained unaddressed. This study focused on spatially outlining the deposits and conservatively ascertaining their gross volume, using combined surface geological mapping and geoelectrical surveying techniques. The geoelectrical surveying aspect comprised 1D geoelectrical (electrical resistivity, spontaneous potential, induced polarization) sounding, and 2D geoelectrical (electrical resistivity and induced polarization) tomographic surveying conducted using ABEM Terrameter (SAS 4000). The 1D electrical resistivity data were processed and interpreted using WinResist version1.0 resistivity inversion software. The 2D geoelectrical tomographic data were processed and interpreted using RES2DINV computer program. The rock outcrops found are quartzose - micaceous as well as graphitic schists, amphibolite, quartzite, coarse grained biotite granite, and exposures of graphite bodies. The graphite bodies are hosted within the schist and quartzite. The schist, amphibolite and quartzite rock bodies appear to be lateral metasediment equivalents, and therefore are synchronous. The geoelectrical attributes of the graphite bodies are 2-90 Ωm resistivity value, combined with 1-20 ms induced polarisation and negative spontaneous potential values. The deposits exist within 0.7 – 12 m depth interval, occupy 1470509.0 m^2 surface area, and constitute 14705090.0 m^3 conservative gross volume. The graphite deposits appear to be sheet like bodies interlaid with the quartzite and schist bodies.

Keywords: Graphite Exposures, Spatially Outlining, Geoelectrical Attributes, Surface Area, Conservative Gross Volume

1. Introduction

Natural graphite is a soft and greasy, steel gray to black, hexagonal carbon allotrope with a metallic lustre and dark gray streak, found deposited in rocks. Its attributes include high thermal stability, high electrical conductivity (or very low electrical resistivity), chemical inertness, elasticity and lubricity [1, 2]. This attribute combination makes graphite an irreplaceable material in manufacturing batteries, refractories, lubricants, brake linings and foundries [3]. It is the commonest anode material in Li-ion batteries employed in electric and hybrid electric vehicles, and in large-scale storage devices such as cellular phones, laptops, and supercapacitors [4-6]. The demand for graphite is spiraling upwards, and the United States and European Union have included it among minerals in critical global supply. Previously economically unattractive graphite deposits now attain ore status [7].

1.1. Definition of the Research Problem

Graphite exposures within Kagara in the North – Central Nigerian Basement Complex were mentioned by Ajibade, A. C. et al [8]. However the specific locations of the individual exposures, their host rocks as well as their spatial extent and

gross volume have hitherto remained unestablished. This study aimed at outlining the Kagara graphite deposits and estimating their gross volume, using surface geological mapping combined with geoelectrical sounding and 2D geoelectrical tomography. It involved (1) producing a location map of the exposures on a scale of 1:15000, (2) ascertaining the range of electrical resistivity, induced polarization and spontaneous potential values that characterise the graphite deposit, and (3) delineating the deposit on a geological map on a scale of 1:15000.

1.2. Location of the Study Area

Kagara is located in North-Central Nigerian Basement Complex, where it lies within latitude N10°10′30" to N10°11'55″ and longitude E6°14′30″ to E6°16′0″ on Nigeria's Tegina Sheet 142 topographic map (Figure 1). It is part of the Birnin Gwari Schist belt.

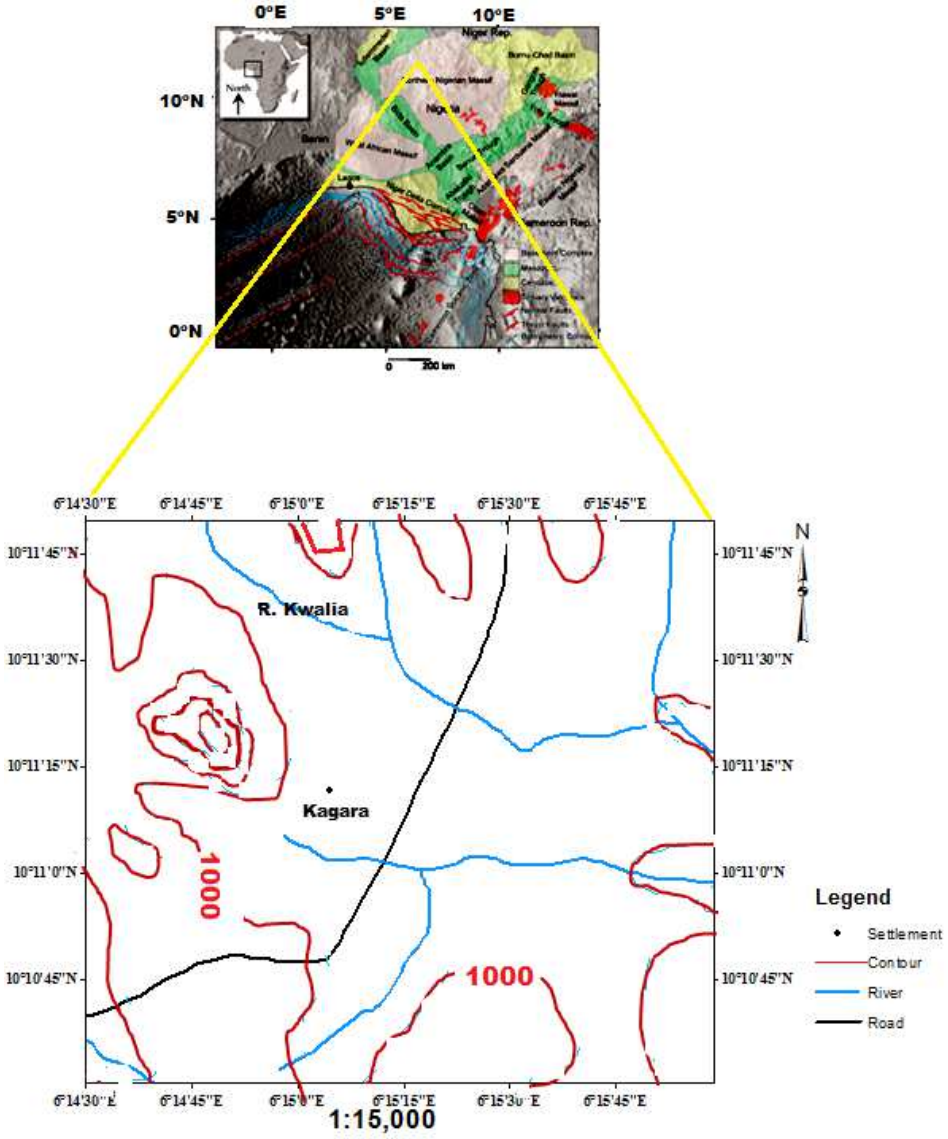

Figure 1. *Study Area.*

2. Materials and Methods

2.1. Theoretical Framework

Graphite occurs within metasediment with protolith organic-rich shales, in plate convergence zones. They are gray, greasy, soft, dark-gray streaked and weathering resistant. This identity facilitates geological mapping of graphite exposures. Continuous graphite bodies are characterised by low electrical resistivity and low induced polarization values. Thus surface resistivity and induced polarization measurements do reveal subsurface graphite targets. 1-D geoelectric sounding models the subsurface as horizontal layers within which resistivity and induced polarization value are constant, but change vertically.

It is thus useful for characterising graphite exposures in terms of geoelectrical attributes. 2-D geoelectrical surveys assumes vertically and horizontally changing resistivity and

induced polarization value, and are thus useful for ascertaining vertical and lateral continuity of graphite exposures.

2.2. Review of Relevant Literature

Existing views on the metasedimentary belts of Nigeria were studied by Nwabufo-Ene, K. E. et al [9]. They expressed that the mineral deposits of the metasedimentary belts had been poorly studied and mildly exploited as chance finds. They employed internal lithological homogeneity and distinctive lithological features, as well as mappability to distinguish six metamorphic rock suites in the North Central Nigeria Basement Complex. The suites are Gneissic Suite, Quartzite Suite, Quartzo – felspathic rock Suite, Pelite Suite, Psammite Suite and Migmatitic Suite. However, they did not associate the rock suites with specific mineralisation. Thus their rock suites were unable to provide prospecting leads in the search for graphite and other mineral deposits in the region. Graphite is included among metallurgical and refractory subgroup of industrial minerals by Rahman, M. A [10]. He emphasised that the level of exploration for mineral deposits in Nigeria is low, and that mineral parageneses of the Nigeria Basement Complex reflect a metamorphic grade that varies from greenschist to amphibolite and granulite facies. However, the work did not associate graphitization with any lithofacies. Surface geological mapping of Minna area in North- Central Nigeria was conducted, and a geological map produced on a scale of 1:250,000 by Ajibade, A. C. [8]. But geological maps that are useful for mineral exploration are those produced on 1:50,000 and larger scales. They found that the rocks in the area include migmatites, high – grade gneisses and schists, as well as low grade schists. They divided the low – grade schist belts on the basis of lithology into Kushaka Schist belt, Ushama Schist belt and Birnin Gwari Schist belt. They found local abundance of graphite within the Birnin Gwari Schist belt, but the specific locations of the graphite deposits were neither given nor were the deposits outlined. The existence of diverse industrial mineral deposits within the metamorphic terrain of the basement complex was acknowledged by Obaje, N. G. [11]. Unlike Nwabufo-Ene, K. E. [8], he recognised that the Birnin Gwari Schist belt contains fine – medium grained quartzo feldspathic rocks that are interbedded with amphibolites and quartzites. But the work did not present the graphite deposits in the belt. The basement geology and mineral belts of Nigeria were reviewed by Haruna, I. V. [12] in order to update existing information on the belts. He noticed that the mineral belts can be divided on the basis of age into Pan African structures (N-S, NNE-SSE) in the western province, and Mesozoic- Early Cretaceous structures (NE-SW and ENE-WSW) on the eastern province. He regarded the mineral belts as linear geologic features in which small low grade epigenetic and or syngenetic mineral occurrences and deposits of a particular paragenesis are found. But he did not associate graphite deposits with any of the mineral belts. Field geological mapping and geochemical investigation of rocks in Kagara area were conducted by Olaolorun, A. O. and Akintola, O. A. [13] to ascertain the origin of rocks that host talc mineralisation in the area. They found that the outcrops in the area comprise migmatitic gneiss, granitic gneiss, meta-arkosic rock, amphibolite, talcose rock, granites, phyllites and pegmatites. They did not report graphite mineralisation in the area.

Many workers [7, 14-18] promote the use of geoelectrical methods in prospecting for ore mineral resources because many ore minerals are electrically conductive, unlike their generally resistive host rocks. Conrad Schlumberger first reported induced polarization phenomenon [19]. The phenomenon was called provoked polarization because potential difference between electrodes failed to drop to zero instantaneously when current was cut off during conventional resistivity measurements. Instead, it dropped sharply at first and then gradually decayed to zero in a time interval. This decay time is now termed chargeability. Integrated geophysical methods were employed by Jalete, A. [20] to prospect for graphite deposits in Gara-Gedemsa area of Mayale in southern Ethiopia. He concluded that the combination of low resistivity values ($\leq$ 10Ωm) with high chargeability values (40 to 70ms) define areas with graphite bodies in Gara-Gedemsa. Geophysical data acquired during exploration for graphite deposit at Uley in Southern Australia were interpreted by Barrette, D. and Dentith, M. [21]. They found that the graphite deposit is conductive and gives low resistivity and negative spontaneous potential values when shallow. They also found that high chargeability values were recorded in areas where there are disseminated graphite bodies. Geophysical and geological investigations were conducted by Ronning, J. S. [22] over graphite occurrences in Vesteralen and Lofoten in northern Norway. They observed spontaneous potential values $\geq$ -100mv above graphite mineralisations. They also established that resistivity values associated with the graphite bodies is $\leq$ 20Ωm in the towns. Subsurface graphite bodies within parts of east coast of Madagascar were delineated by Heritiana, A. R. [23] using self-potential (SP), electrical resistivity tomography (ERT) and induced polarization (IP) methods. They recorded negative SP values with low electrical resistivity and high chargeability in areas where graphitic content is >5%. According to Khalid, S. E. and Munschy, M. [24], mineral exploration is vital in many countries to increase the income of their people, and their economy relies upon discovering minerals. They remarked that the combination of passive methods (SP) with active methods (electrical resistivity, and induced polarization) do capture subsurface ore targets. They concluded that the combination of two or more approaches certifies much more consistent results.

2.3. Field Data Acquisition, Processing and Interpretation Procedures

Fresh samples of rock outcrops were identified in the field and given field petrological names, on the basis of texture and MCI (Mafic Colour Index). MCI is the percentage of visible mafic minerals (green, dark gray, black minerals) in the rocks. Strike, dip direction and dip amount of foliated

rocks were determined using a compass-clinometer. Representative samples were thin sectioned, and petrographic analysis was performed on them. The field petrological names were fine-tuned and the rock types established. Graphite exposures were identified using their low weight, opaque nature, gray – black appearance, hardness of 1-2 on Mohr hardness scale, greasy feel and dark gray streak. Geographical coordinates of locations of the graphite exposures and other identified rock outcrops were obtained using *etrex* version of hand held GPS (Geographic Position System). Using the coordinates, locations of the graphite exposures and other identified rock outcrops were plotted on a field base map (fact map) produced on a scale of 1:15000 from Tegina Sheet 142 topographic map of Nigeria. Thus outcrops location map was produced.

1D and 2D geolectrical data were used to characterize the graphite bodies electrically. ABEM Terrameter (SAS 4000) was employed in the geoelectrical data acquisition. 1D resistivity, induced polarization (IP) and spontaneous potential (SP) sounding were conducted in the vicinity (about 0.30 m offset distance) of a graphite outcrop. The Schlumberger field geometry was employed with acquisition electrodes arrayed along a 200 m traverse in the outcrop strike (N-S) direction. The 1D resistivity sounding data was processed and interpreted using WinResist version 1.0 for 1D resistivity data inversion. The measured one dimensional IP and SP values were plotted against electrode spacing using Micosoft Excel. Some workers [17, 25, 26] gave the resistivity values of weathered bedrock (overburden), graphite bodies, schist and quartzite as 100-1000 Ωm, 10-100 Ωm, 50-1000 Ωm and 100-200000 Ωm respectively. Using these values as a guide, discontinuities were related to subsurface intervals of overburden, graphite bodies and fresh basement. The 2D geoelectrical data for characterizing the graphite bodies was acquired using the Werner Alpha geometry with sixteen electrodes arrayed along 30 m traverse along strike of rock outcrops. The minimum electrode spacing for the measurement was 2 m. The spacing was consecutively expanded in multiples of 2, 3, 4 and 5, thereby giving six data levels and a total of 35 data points.

Two 2D geoelectrical resistivity and induced polarization surveying were also conducted between the graphite and other rock outcrops, along overburden covered 200 m traverse in outcrop dip direction. This was to ascertain subsurface continuity of the graphite bodies because lithologic units do change along dip direction. The survey employed 21 electrodes, and 5 m minimum electrode spacing which was expanded consecutively in multiples of 2, 3, 4 and 5 to give 6 levels of measurement and 63 data points. The 2D geoelectrical data were processed and interpreted using RES2DINV computer program.

Spatial disposition of the mapped rocks was completed on the outcrop location map, using the strike and dip direction of the foliated rocks. Inferred subsurface graphite bodies were combined with the graphite outcrop locations to delineate spatial extent of the graphite deposits within the rock outcrop map. Thus the geologic map was produced on the 1:15000 scale. The area of the delineated spatial extent was estimated manually. The gross volume of the graphite body was estimated as product of the average its area and average thickness obtained from the geoelectrical plots.

3. Results and Discussion

3.1. Field Geological Aspect

Rock outcrops found are schist, amphibolite, quartzite and granite. The schist bodies are micaceous (M), quartzose (Q) and contain opaque bodies (OPQ) – Figures 2, 3 and 4. They generally strike NNW-SSE (352°) and dip 25°westwards.

Figure 2. *Micaceous and quartzose schist (N10°10'45"; E6°15'15").*

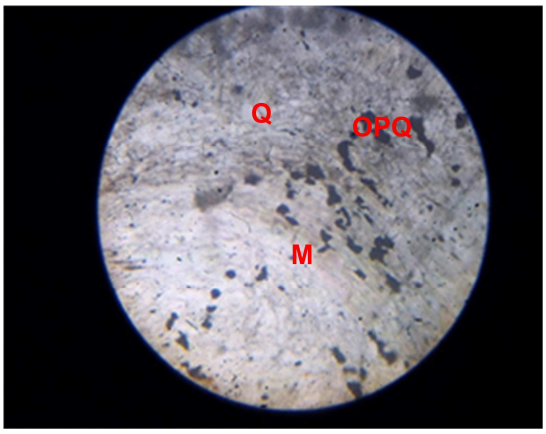

Figure 3. *(PP M100).*

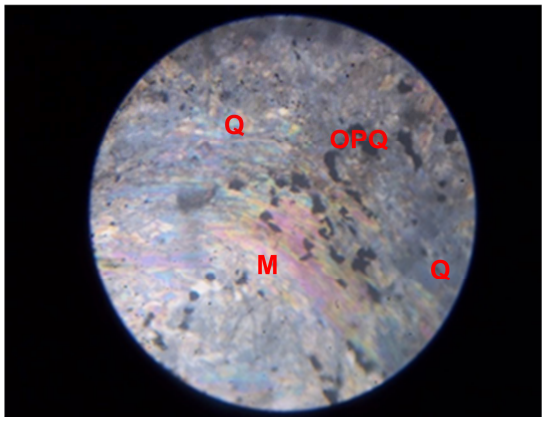

Figure 4. *(XP M100).*

Some of the schist bodies are graphitic (Figure 5).

Figure 5. *Graphitic schist body (N10°11'18.12"; E6°15'40.8").*

The amphibolite bodies are banded and greenish gray in appearance (Figure 6). They contain amphibole (AMP), muscovite (M) and little quartz (Figures 7 and 8). Like the schist, they generally strike NNW-SSE (352°) and dip 25° westwards.

Figure 6. *Banded Amphibolite outcrop (N10°11'44.11"; E6°15'53.72").*

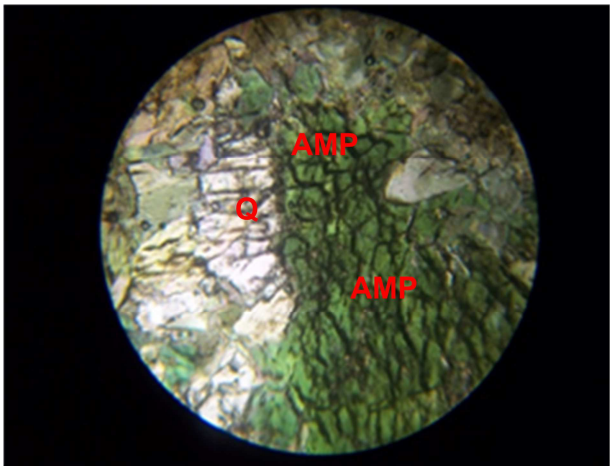

Figure 7. *PP M40.*

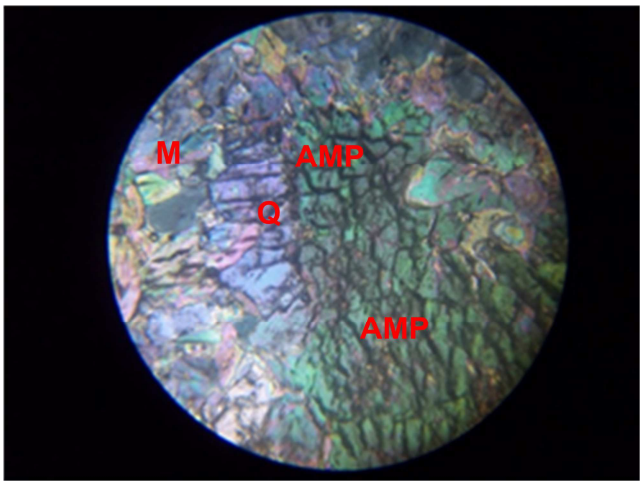

Figure 8. *XP M40.*

Figure 9 is one of the quartzite outcrops.

Figure 9. *Quartzite outcrop (N10°11'22.31"; E6°15'39.44").*

Figure 10 is an exposure of graphite, while Figure 11 is an exposure of graphite intercalated with quarzite.

Figure 10. *Graphite Exposure (N10°11'22.39"; E6°15'40.27").*

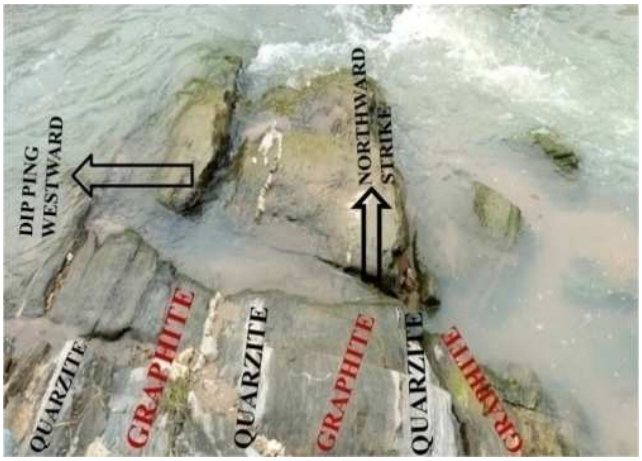

Figure 11. *Exposure of graphite and quartzite intercalation (N10°11'36.62"; E6°15'40.08").*

The parallelism in structural attitude between schist and amphibolite suggests they are lithofacies equivalent, and therefore are synchronous rock bodies. Graphitic schist bodies, as well as observed intercalation of quartzite and graphite bodies, indicate graphitization of protolith organic bearing shales and clays that were intercalated with sandstone in some places. Thus the schist, amphibolite, quartzite and graphite bodies appear synchronous. Figure 12 shows coarse grained granite with schist xenoliths. The xenoliths indicate the granite intruded the schist body, and therefore the granite is younger.

Figure 12. *Coarse grained granite with xenolith of schist (N10° 10' 54.08"; E6° 15' 20.14").*

The mineral constituents of the granite are biotite (B), quartz, muscovite (M) and orthoclase (ORT)- Figures 13 and 14.

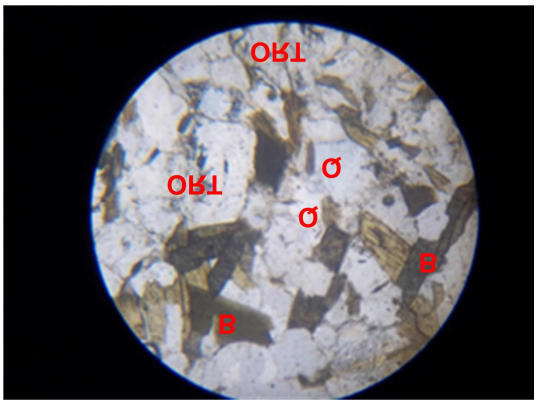

Figure 13. *PP M100.*

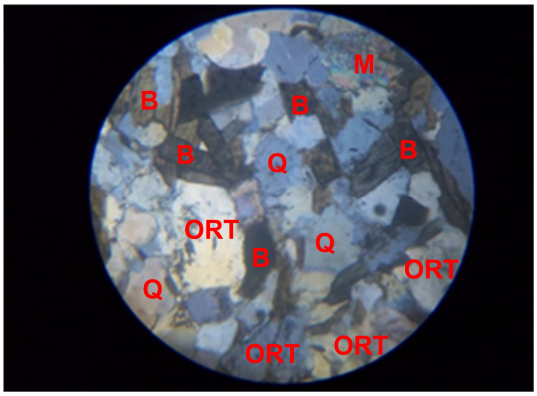

Figure 14. *XP M100.*

The rock outcrop location map is Figure 15. The outcrop map suggests that the graphite bodies are interlaid within schist and quarzite bodies.

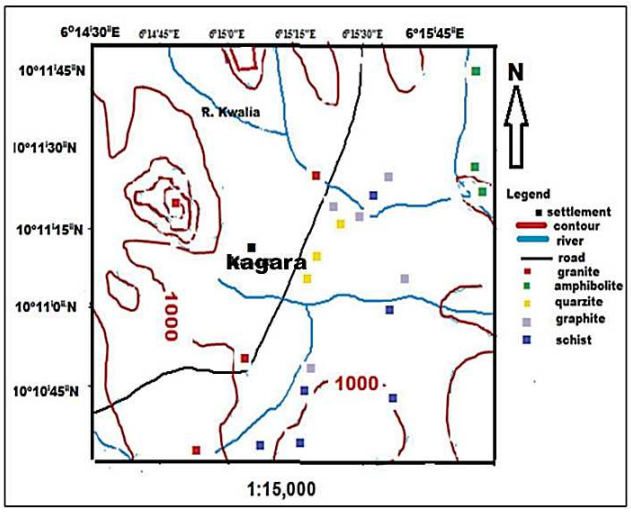

Figure 15. *Rock outcrop locations.*

3.2. Surface Geoelectrical Aspect

Figures 16, 17 and 18 are respectively the results of 1D resistivity, SP and IP sounding conducted (at Latitude N10°11'40.78" and Longitude E 6°15'30.22") in the vicinity of a graphite outcrop.

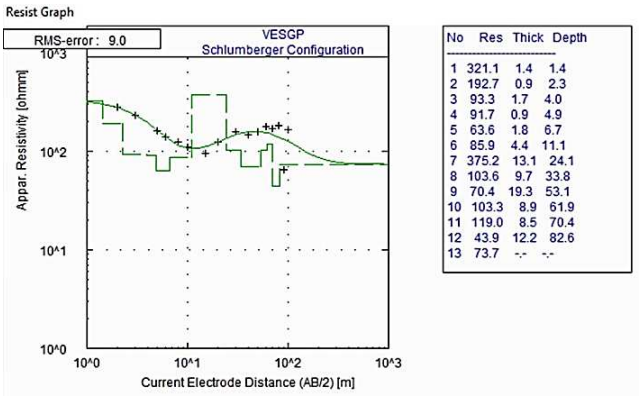

Figure 16. *1D subsurface resistivity model (N10°11'40.78"; E6°15'30.22").*

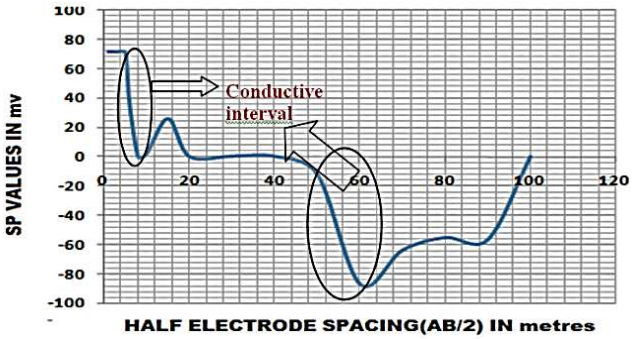

Figure 17. *SP sounding curve (N10°11'40.78"; E6°15'30.22").*

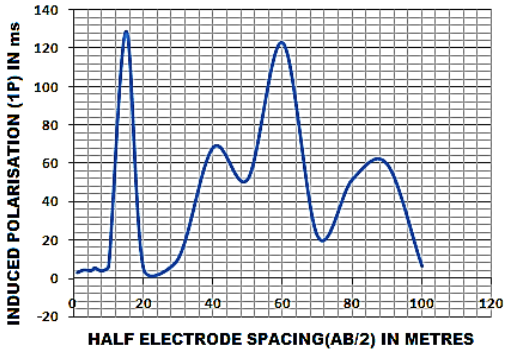

Figure 18. *IP sounding curve (N10°11'40.78"; E6°15'30.22").*

The 1D subsurface resistivity model (Figure 16) presents resistivity values of 93.3 to 63.6 Ωm between 3.0 – 11.1m depth. This reflects a continuous graphite body within the depth interval. The drop in SP values from 72.0 to -0.2 mv within this depth interval supports the presence of a continuous conductive body observed to be graphite on the surface. Barrette, D. and Dentith, M. [21] found similar pattern of low resistivity and sharp drop in SP values associted with massive graphite deposits in Uley in South Australia. The IP values range from 0-4 ms in the depth interval. Jalete, A. [20] measured such low values of electrical resistivity and chargeability within continuous graphite bodies in Gara-Gedemsa area in Southern Ethiopia.

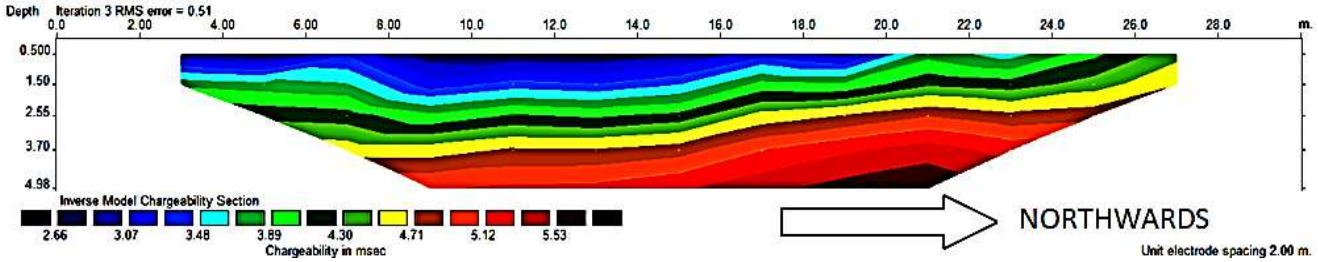

Figure 19. *2D subsurface IP model along strike (N-S traverse), passing through electrode position 14, station (N10°11'40.78"; E 6°15'30.22").*

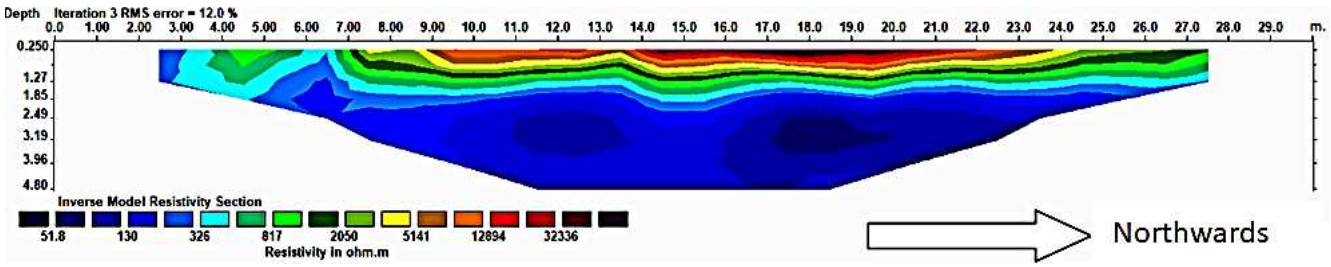

Figure 20. *2D subsurface resistivity model along strike (N-S traverse), passing through electrode position 14, station (N10°11'40.78"; E 6°15'30.22").*

Figures 19 and 20 are respectively 2D subsurface chargeability (IP) and resistivity models employed with the 1D geoelectrical information to characterise the graphite body in terms of geoelectrical attributes.

The 2D models show parallel subsurface geoelectric layers aligned northwards, which confirms that the acquisition traverse was along strike. The 1D geoelectric sounding station coincides with 14 m electrode position on the 2D models. At this position, chargeability increases (from 3.0 to 5.0 ms) and resistivity decreases (from 320.0 to 50 Ωm) within 2.2 to 4.50 m depth interval on the 2D models. This is the interval occupied by the continuous subsurface graphite body. Figures 21 and 22 respectively are 2D subsurface resistivity and IP models obtained from 2D geoelectrical traverse across strike (East-West) at the 1D sounding station. The 2D subsurface resistivity model (Figure 21) reveals very low resistivity (2.0 - 50 Ωm) intervals at 35-50 m, 75-77 m and 88-100 m electrode positions along the eastward

traverse. The IP values (Figure 22) at these positions are generally < 5 ms. The combination of low resistivity with low IP at these positions indicates deposits of continuous graphite bodies. The bodies lie generally within 0.7 - 12.0 m depth interval. The comparatively high resistivity (200 - 400 Ωm) and low IP (9 - 18 ms) intervals that separate the graphite bodies are inferred to be quartzite bodies. Similar resistivity values were associated with graphite and quartzite by Kearey, P. [17], Milsom, J. [25] and Reynolds, J. M. [26]. This inference is in agreement with intercalations of graphite and quartzite bodies along dip traverse (East-West direction) observed on the surface, as shown in Figure 11.

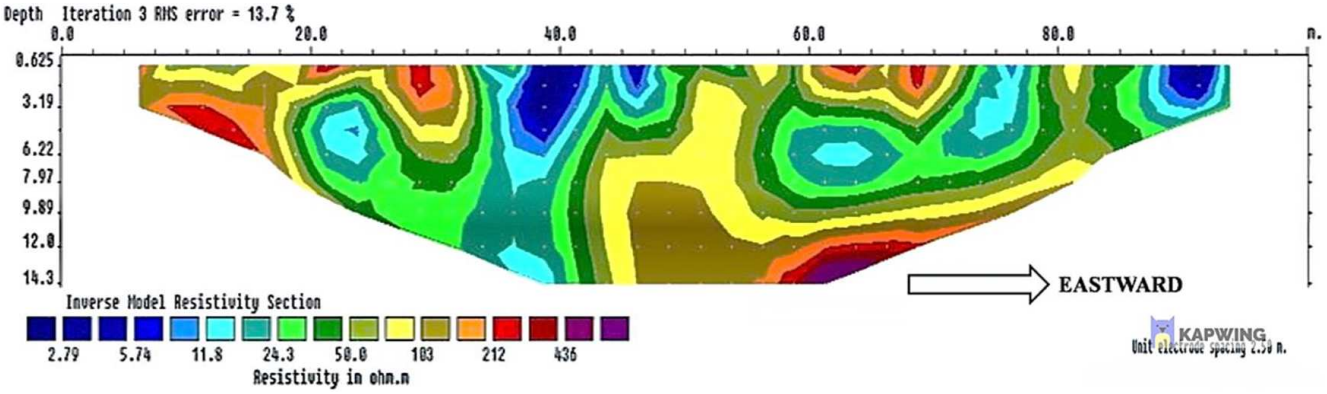

Figure 21. *2D subsurface resistivity model obtained from 2D geoelectrical traverse across outcrop strike (East-West) at the 1D sounding station (N10°11'40.78"; E 6°15'30.*

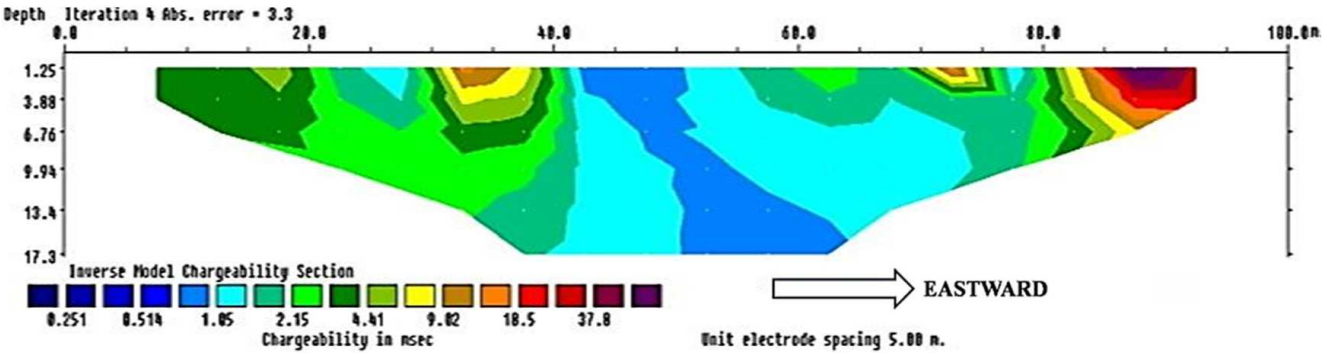

Figure 22. *2D subsurface IP model obtained from 2D geoelectrical traverse across outcrop strike (East-West) at the 1D sounding station (N10°11'40.78"; E 6°15'30.*

The 2D subsurface resistivity model (Figure 21) reveals very low resistivity (2.0 - 50 Ωm) intervals at 35-50 m, 75-77 m and 88-100 m electrode positions along the eastward traverse. The IP values (Figure 22) at these positions are generally 1 - 20 ms. The combination of low resistivity with low IP at these positions indicates deposits of graphite bodies. The bodies lie generally within 0.7 - 12.0 m depth interval. The comparatively high resistivity (200 - 400 Ωm) and High IP (≥ 30 ms) intervals that separate the graphite bodies are inferred to be quartzite bodies. This inference is in agreement with intercalations of graphite and quartzite bodies along dip traverse (East-West direction) observed on the surface, as shown in Figure 11.

Figures 23 and 24 respectively are 2D subsurface resistivity and IP models along traverse in outcrop dip direction that passes through the location with coordinates N10°11'44.35 "N, E6°15'43.27".

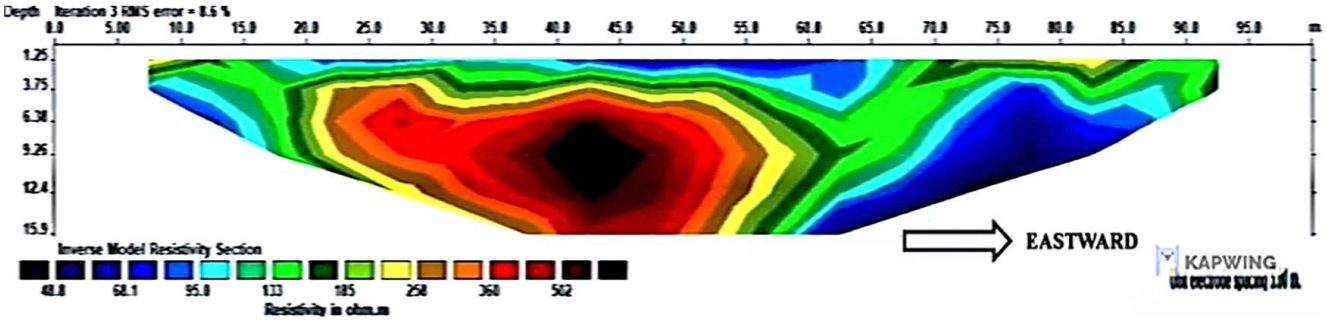

Figure 23. *2D subsurface resistivity model along outcrop dip traverse (East-West direction) through location N10°11'44.35 "N, E6°15'43.27".*

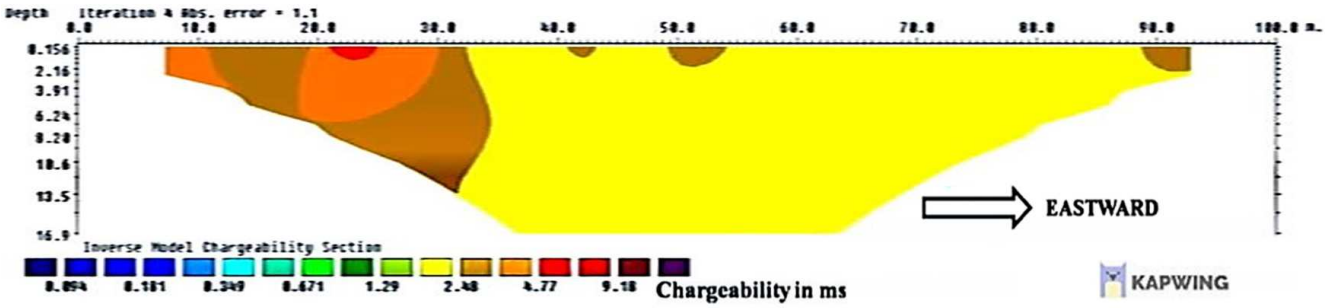

Figure 24. *2D subsurface IP model along outcrop dip traverse (East-West direction) through location N10°11'44.35 "N, E6°15'43.27".*

The subsurface resistivity (Figure 23) generally ranges from about 40 - 100 Ωm along the entire traverse within 1.5 to 6.0 m depth interval. Towards the eastern end of the traverse, the resistivity is consistently lower than 95 Ωm within 3.8 to 15.9 m depth interval. This indicates that the graphite body exists throughout the traverse. The IP values (Figure 24) range from 2.0 to 9.0 ms along the traverse, thus supporting the existence of continuous subsurface graphite body. Figure 25 shows the outlined graphite deposit within the other rock units. This occupies an estimated surface area of 1470509.0 m^2, which multiplies with its average thickness of 10.0 m to give an estimated conservative gross volume of 14705090.0 m^3 graphite deposit.

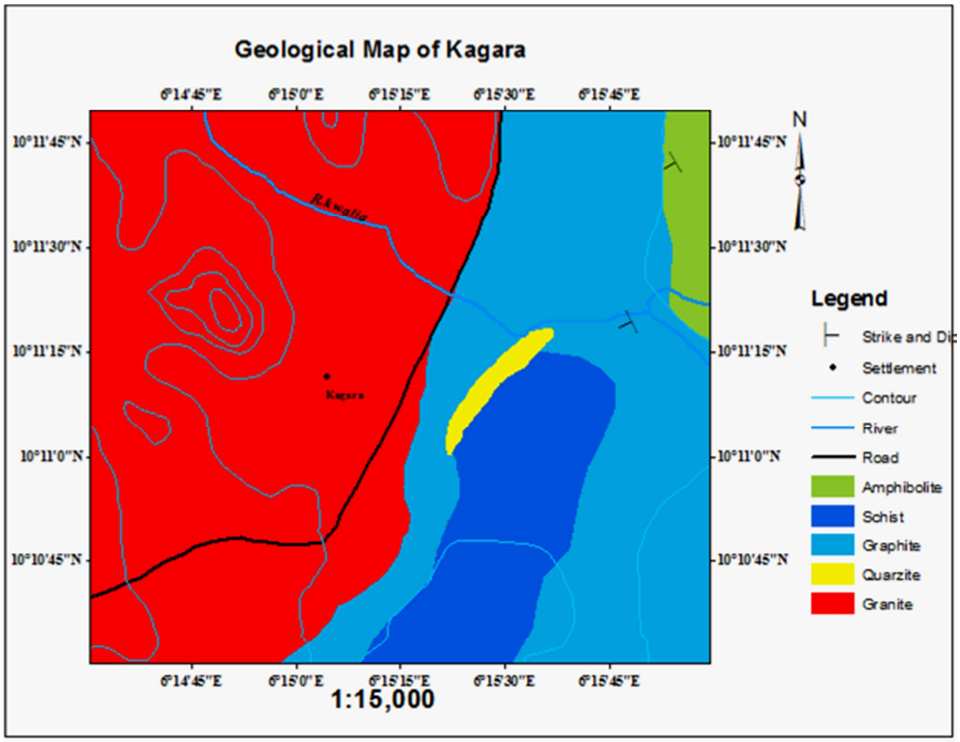

Figure 25. *Spatial extent of graphite deposit within rock outcrops in Kagara.*

4. Conclusion

The combination of lithologic mapping with 1D geoelectric sounding and geoelectric tomography enabled the geo-electrical characterization, spatial delineation and conservative estimation of the gross volume of graphite deposit in Kagara. The subsurface deposit was identified by combination of 2 – 90 Ωm resistivity with 1-20 ms IP and negative SP anomaly. The deposit exists within 0.7 - 12 m depth interval, and has an average thickness of about 10.0 m. It occupies a spatial extent of about 1470509.0 m^2 and constitutes a conservative gross volume of about 14705090.0 m^3. The deposit appears to exist as a series of sheet-like bodies interlaid with quarzites.

The development of this deposit and other graphite deposits in Nigeria will generate employments and additional revenue in the country.

References

[1] Anthony, W. Bideaux, R. A., Bladh, K. W. and Nichols, M. C., (2003). Handbook Of mineralogy (1): elements, sulphides, sulfosalts. Mineral Data Publishing, Tusco, Arizona.

[2] Wissler, M. (2006). Graphite and carbon powder for electrochemical applications. Journal Of power sources, 156, 142-150.

[3] Shaw, S., 2013. Graphite demand and growth: the future of lithium-ion batteries in EVs and HEVs, Proceedings of 37th ECGA General Assembly.

[4] Yoo, H. D., Markevich, E., Salitra, G., Sharon, D. and Aurbach, D (2014). Materials today, 17 (3), 110-120.

[5] Dickson, J. S., 2014. Talga eyes graphene potential. Industrial minerals, 567: 35-36.

[6] Simandl, G. J., Pardon, S and Akam, C., 2015. Graphite deposit types, their origin and economic significance. In: Simandl, G. J. and Nextz, M. (eds.) Symposium on strategic and critical mineral proceeding, November 13-14, Victoria, British Colombia British Colombia Geological Survey paper 2015-3, p163 - 171.

[7] Meunier, E. (2015). Exploring for Graphite Using a New Ground Based Time Domain Electromagnetic System, Carleton University, M.Sc Thesis, Canada.

[8] Ajibade, A. C., Anyanwu, N. P. C., Okoro, A. U., and Nwajide C. S., 2008. The Geology of Minna area, Bulletin 43 of Nigerian Geological Survey Agency.

[9] Nwabufo-Ene, K. E. and Mbonu, W, C. (1988). The metasedimentary belts of the Nigerian Basement Complex – Facts, Fallacies and new Frontiers. In: Precambrian Geology of Nigeria. Eds: Oluyide, P. O., Mbonu, W. C., Ogezi, A. E., Egbuniwe, I. G., Ajibade, A. C., Umeji, A. C., pp 35-65.

[10] Rahman, M. A., 1988. Recent advances in the study ofbasement complex of Nigeria: In P.O. Oluyide (Co-ordinator); Precambrian Geology of Nig. Geol. Surv. Nig. Publ., 11-43.

[11] Obaje, N. G. (2013). Updates on the geology and mineral resources of Nigeria. Onaivi printing and publishing Co, Abuja, 213 p.

[12] Haruna, I. V. (2017). Review of Basement Geology and Mineral Belts of Nigeria. IOSR Journal of Applied Geology and Geophysics, 5 (1), 37-45.

[13] Olaolorun, A. O. & Akintola, O. A. (2018). Compositional Characteristics in Relation to the Evolution of Granite Suites in Guguruji Area, Parts of Ayetoro (Sheet 226 NW and NE) and Kagara, Tegina (Sheet 142 SE), North-Central, Nigeria. International Research Journal Of Advanced Engineering and Science, 3 (1), 80-90, 2018.

[14] Keller, G V and Frischknecht, F C (1966), Electrical Methods in Geophysical Prospecting, Pegamon, Press, Oxford.

[15] Parasnis, A S (1986), Principles of Applied Geophysics, Chapman and Hall, London.

[16] Lowrie, W (1997), Fundamentals of Geophysics, Wiley and Sons, Cambridge.

[17] Kearey, P., Brooks, M. and Hill, I., 2002. An Introduction to Geophysical Exploration, Blackwell Scientific, Oxford, UK.

[18] Baranwal, V. E., Ronning, J. S, Gautneb, H., Larsen, B. E. Ofstad, F., & Bronner, M (2018). Integrated interpretation of airborne and ground geophysical data for graphite exploration in Northern Norway. Abstract: 24th Induction workshop. Helsinger, Denmark, August 12-19.

[19] Dobrin, M B. and Savit, C H (1988), Introduction to Geophysical Prospecting, McGraw-Hill, New York.

[20] Jalete, A. (1997). Application of Integrated Geophysical Methods for Graphite Exploration in Gara-Gedemsa Area, South Ethiopa. Unpublished M.Sc Thesis, Addis-Ababa University, Ethiopia, 86p.

[21] Barrette, D. & Dentith, M. (2003). Geophysical Exploration for Graphite at Uley, South Australia. ASEG Extended Abstracts, 3, 47-8. Doi: 10.1771/ASEGSpec 1204.

[22] Ronning, J. S., Gautneb, H., Larsen, B. E., Knezevic, J., Baranwal, V., Elvebakk, H., Gellein, J., Ofstad, F., & Bronner, M. (2017). Geophysical and geological investigations of graphite occurrences in Vesterålen and Lofoten, Northern. NGU-rapport 2018.011.

[23] Heritiana, A. R., Riva, R. Ralay, R., & Boni, R. (2019) Evaluation of flake graphite ore using self-potential (SP), electrical resistivity tomography (ERT) and induced polarization (IP) methods in east coast of Madagascar, Journal of Applied Geophysics 169 (9). doi: 10.1016/j.jappgeo.2019.07.001.

[24] Khalid, S. E. & Munschy, M. (2019). Introductory Chapter: Mineral Exploration from the Point of View of Geophysicists. Minerals, Intech Open, 10.5772/ in techopen.84830.hal-03105786.

[25] Milsom, J., 2003. Field Geophysics, 3rd Edition, John Wiley and Sons, UK.

[26] Reynolds, J. M., 2011. An Introduction to Applied and Environmental Geophysics, 2nd edition, Wiley-Blackwell, Oxford.